captured by first looking past the paper at some object about three times as far from the eye as the views are, seeing the three views out of the bottom of the eyes, and then finally focusing on the middle view. It takes an appreciable time for the final focus to become effective. Horizontal alignment is essential.

References

[1] French, T. E. and Vierck, C. J., *A Manual of Engineering Drawing* (McGraw-Hill Book Company, Inc., New York, 1953), 8th ed., Chaps. 10, 11, 16, and 17.

[2] Martin, L. C., *Technical Optics* (Sir Issac Pitman and Sons, London, 1954), Vol. 2.

JANUARY 1964 J. SPACECRAFT VOL. 1, NO. 1

Impact of Dislocation Theory on Engineering

JOHN E. DORN* AND JACK B. MITCHELL†
University of California, Berkeley, Calif.

Dislocation theory is discussed in terms of the nature and properties of individual dislocations and their interactions. Examples are given illustrating how dislocation theory permits a description of the mechanical behavior of crystalline materials in terms of mathematical, physical, and chemical concepts familiar to engineers. Although the paper presents several direct results of the application of dislocation theory to the development of engineering materials, the major emphasis is given to the value of dislocation theory in the development of a sound philosophical background and simple analytical procedures for the development of new crystalline materials and for predicting how real materials might behave under new and different environmental conditions.

Introduction

HINTS concerning the possible importance of some dislocation-like imperfections in crystalline materials were announced in 1928 and 1929 by Prandtl[1] and Dehlinger.[2] In 1934 Taylor,[3] Orowan,[4] and Polanyi[5] independently "invented" models of slip dislocations on which the presently accepted dislocation theory is based. Progress in extending this new engineering science was extremely slow prior to 1948. This delay might, in part, be attributed to interruptions by World War II, but it was principally because 1) no one had truely "seen" dislocations except in terms of very indirect evidence, and 2) several different investigators could marshall evidence to "describe" the same experimental facts in terms of several unique and often apparently contradictory dislocation models. It is now recognized that dislocations are extremely versatile, a fact that stimulates the imagination and warns against hasty and naïve interpretations.

Since 1948 great progress has been made in our grasp of the subject of dislocations: 1) dislocations can now be "seen" in a number of ways: 2) a vast body of sound theory has been generated; and 3) a host of experimental observations can now be uniquely and accurately analyzed in terms of the theory. On the other hand, much yet needs to be done before a full and accurate account of all issues can be presented, and because dislocations are so versatile, theory and experiment must yet be advanced simultaneously, each complementing the other in arriving at the truth.

Dislocation theory has been, and is currently being, applied toward the development of new alloys. It has led to the development of nonstrain-aging automotive sheet and to the development of extremely high-strength ausformed steels, and it is now being applied to the development of new creep-resistant alloys of the refractory metals and to the possible production of ductile ceramics. Such direct examples of applications are easily appreciated. However, there is another perhaps greater, but less obvious, significance of dislocation theory to the engineer: It gives him a sound analytical basis in terms of atomistics and the mathematical theory of elasticity on which to base his judgment not only regarding the development of new crystalline materials having special desirable properties but also with respect to predictions of how real materials might behave under new and different environmental conditions. It will help him to decide whether or not the plastic behavior of a new material will be temperature- or strain-rate sensitive and whether the flow stress will be so high at low temperatures that notch-sensitivity and brittleness may be imminent, and it will provide the basis for formulating the constitutive equations essential to the solution of problems of deformation of materials.

Since this paper is being written primarily for those engineers who have only a modest background in the subject, some of the elementary concepts on the nature of dislocations, their stress fields, and energies will be reviewed before other more sophisticated problems are illustrated.

Nature of Dislocations

As shown in Fig. 1, the theoretical resolved shear stress τ for slip in an ideal single crystal is 10% of the shear modulus of elasticity. Extremely small whiskers of metallic and

Presented as Preprint 63–236 at the AIAA Summer Meeting, Los Angeles, Calif., June 17–20, 1963; revision received October 21, 1963. The authors express their appreciation to the U. S. Atomic Energy Commission for their support of this research conducted under the Inorganic Materials Research Division of the Lawrence Radiation Laboratory in Berkeley. They further wish to thank Jim Mote for his advice and help in preparing this paper.

* Miller Professor of Materials Science 1962–63, Department of Mineral Technology; also Research Metallurgist, Inorganic Materials Research Division, Lawrence Radiation Laboratory.

† Research Metallurgist, Inorganic Materials Research Division, Lawrence Radiation Laboratory.

ceramic crystals occasionally approximate this strength, suggesting that they are ideal, but many pure single crystals begin to deform plastically at 10^{-4} to 10^{-3} of this value and are therefore imperfect. Crystals can exhibit point, line-of-surface imperfections (Fig. 2), but only the line imperfection known as a dislocation can account for slip on a slip plane in a slip direction. The unit motion of a dislocation is shown in Fig. 3. In contrast to slip in the ideal crystal (Fig. 1), where all atoms on the slip plane move in unison, only small readjustments of atom positions in the vicinity of the core of the dislocation are required to cause slip in the real crystal (Fig. 3).

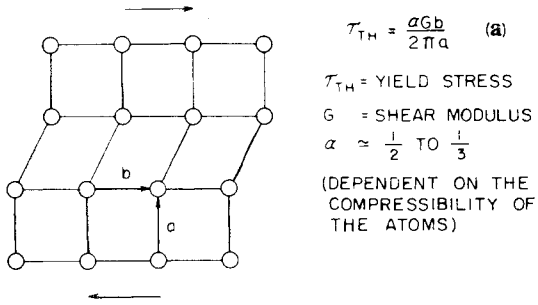

Fig. 1 Yield stress in an ideal metal (materials: metallic and ceramic whiskers about 1-μ diam).

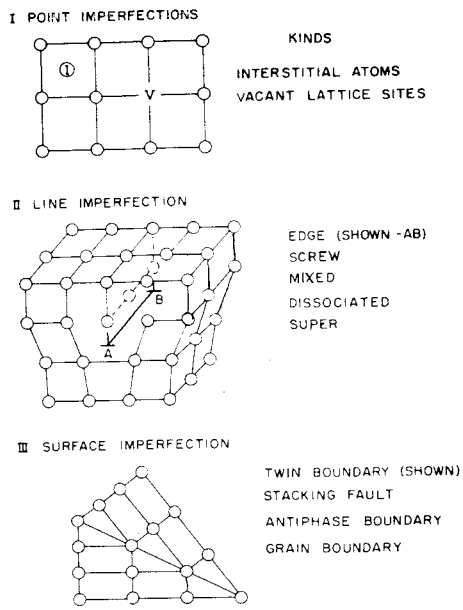

Fig. 2 Crystal imperfections.

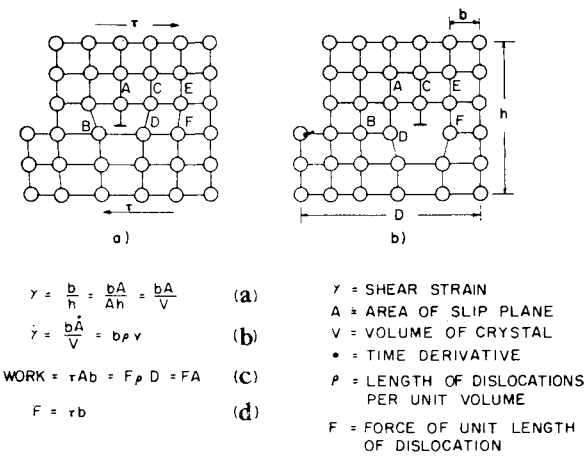

Fig. 3 Motion of dislocations.

For this reason a real crystal often has low yield strength but can be made quite strong by imposing barriers to the motion of dislocations in the form of other dislocations, solute atoms, or dispersed particles.

A general dislocation is shown in Fig. 4a, where we have conceived the dislocation to be born at a point of stress concentration so as to sweep out the cross-hatched area. The dislocation line $ABCD$ demarks the region that was displaced by the Burgers vector b in the slip direction from the unslipped portion of the crystal. An extra half plane of atoms was crowded into the region above AB which is now an edge dislocation (Fig. 2). The edge dislocation line AB is normal to its Burgers vector b, so that the Burgers vector and the line define the slip plane. Segment CD, shown as a plan view of atomic positions in Fig. 4b, is a screw dislocation where the atoms form a spiral ramp around the dislocation line. Since a pure screw dislocation is parallel to its Burgers vector, it cannot be associated with a specific slip plane; hence it can cross-slip from one plane to another. Segment BC is a mixed dislocation having both edge and screw components. Since slip dislocations are lines that demark slipped from unslipped regions, they must either terminate on the surface of the crystal or form closed loops, and the Burgers vector, which is the atomic slip distance, must be constant along the total length of the dislocation. Dislocations can be "seen" by various techniques. Figure 5 shows a typical three-dimensional Frank network of dislocations as revealed by thin film

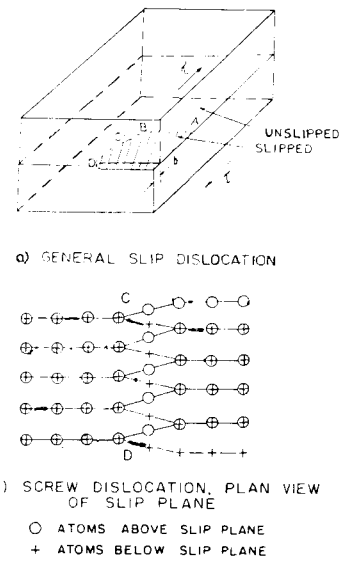

Fig. 4 General slip dislocation.

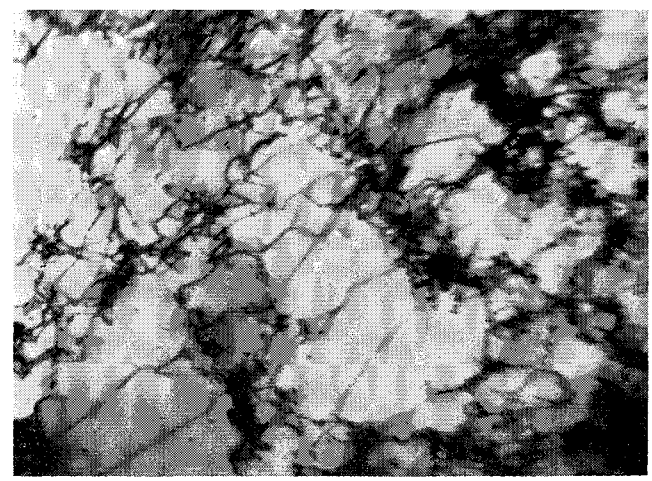

Fig. 5 Transmission electron micrograph of Cu strained about 10% illustrating the dislocation network and the beginning of the formation of dense entanglements in cells. Courtesy of J. Washburn.

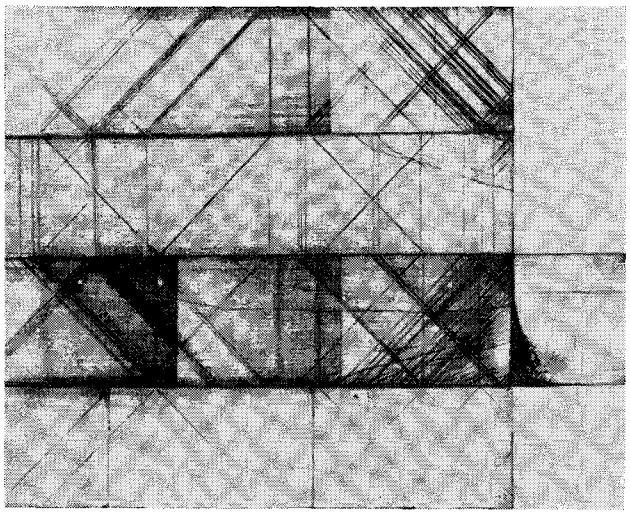

Fig. 6 Single crystal of MgO which was strained plastically and etched. Arrays of dislocations can be seen in intersecting slip bands. Courtesy of J. Washburn.

electron transmission microscopy. Figure 6 is a deformed and etched crystal of MgO showing a series of etch pits at points where dislocations on slip bands intersect the surface of the crystal. Other techniques, such as absorption of infrared light in Si at dislocations decorated with Cu, have been used to "see" dislocations.

Stress Fields and Dislocation Energies

A most interesting feature of dislocation theory arises from the fact that it permits the rationalization of the plastic behavior of crystalline materials in terms of the theory of elasticity. Dislocations, such as CD in Fig. 4b, are the center of a region of elastic deformation in the crystals; consequently, plastic deformation arises only from the motion of such elastic strain centers. Such contained elasticity for continuum mechanics was discussed by several elasticians long before the advent of dislocation theory; for example, important contributions were made as early as 1907 by Volterra[6] in his analyses on "distortioni." Several more pertinent accounts of the mathematical theory of dislocations have now been published.[7–10]

The shear strain γ a distance r from the center of a screw dislocation is readily estimated to be $b/2\pi r$, since the ramp of atoms advances b for one complete circuit.[11] Consequently, the shear stress is $\tau = Gb/2\pi r$. As shown in Fig. 7a, two dislocations of opposite sign on the same slip plane will attract and annihilate each other, since the total strain energy is reduced when this happens. When a stress τ is applied, the positive dislocation moves to the right and negative to the left, as shown in Fig. 7b. The stress necessary to make them separate must overcome their mutual attractions and therefore exceed $\tau^* = Gb/4\pi y$. Thus, as a metal is strained and more dislocations are introduced, y decreases, resulting in one of the several contributing mechanisms of strain hardening.

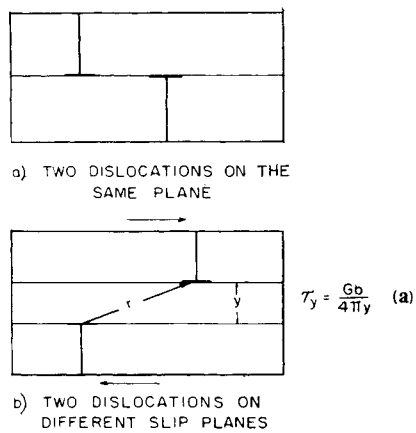

Fig. 7 Interaction stresses between dislocations.

Table 1 Dislocation processes

Class	Characteristics
1) Athermal and velocity insensitive examples: a) Long-range stress fields b) Short-range and long-range ordering in alpha solid solutions c) Suzuki-locked alloys	Activation energies that are greater than 50 kT and therefore cannot be thermally activated. Deformation stresses that are independent of the strain rate and insensitive to the test temperature, usually $\tau = \tau\{\gamma\}$ (a)
2) Thermally activated examples: a) Peierls process b) Intersection c) Cross-slip for dissociated dislocations d) Climb of edge dislocations e) Viscous creep due to solute atom interactions	Activation energies are less than 50 kT. Flow stresses that decrease rapidly with an increase in temperature or a decrease in strain rate. Creep processes: $\dot{\gamma} = f^{+}\{\tau,str,T\}e^{-u^{+}\{\tau,str,T\}/kT} - f^{-}\{\tau,str,T\}e^{u^{-}\{\tau,str,T\}/kT}$ (b)
3) Athermal but velocity-sensitive examples: a) Relativistic motion of dislocations[15] b) Phenon interactions with moving dislocations[16]	Not thermally activated but yet exhibiting an effect of strain rate on the stress: $\dot{\gamma} = \frac{10}{3}\frac{\rho bc\tau}{kT}$ (c)

One of the most significant features of a dislocation is its energy[12]; this is the strain energy Γ induced in the crystal lattice as a result of the dislocation. If we consider a unit length of a screw dislocation, the strain energy per unit volume at a distance r from the core of the dislocation is

$$d\Gamma/2\pi r dr = \tau\gamma/2 = Gb^2/2(2\pi r)^2 \tag{1}$$

For the usual geometric conditions that prevail in establishing the boundary conditions, the integral of this equation suggests that the energy per unit length of a dislocation is approximately

$$\Gamma = 0.5Gb^2 \tag{2}$$

Dislocation Mechanisms

The mechanisms that dislocations[13] can undertake are conveniently classified into three major groups (Table 1).

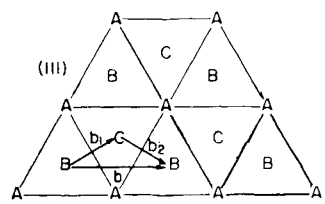

a) $\mathbf{b} \rightarrow \mathbf{b}_1 + \mathbf{b}_2$ (a)

b) $\Delta U \cong \frac{G}{2}(\bar{b}_1 \cdot \bar{b}_1 + \bar{b}_2 \cdot \bar{b}_2 - \bar{b} \cdot \bar{b}) = \frac{Ga^2}{2}(\frac{6}{36} + \frac{6}{36} - \frac{2}{4})$

$= \frac{-Ga^2}{12}$ (b)

Fig. 8 Atomic arrangement and burgers vectors in *FCC* crystals.

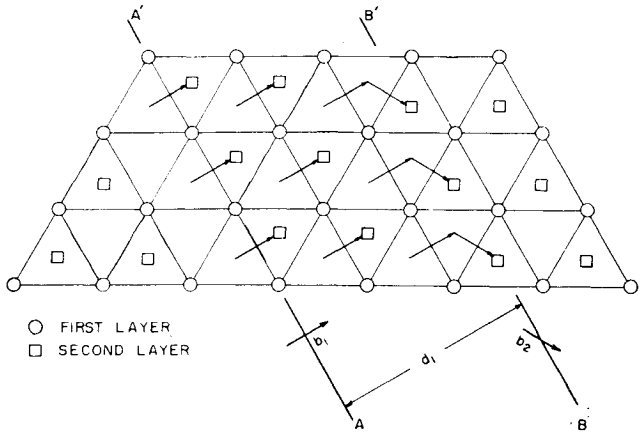

Fig. 9 Partially dissociated dislocation.

Occasionally, only one of these mechanisms controls the plastic deformation, but usually several are operative at one time. As shown by Eq. (a) of Table 1, the athermal processes generally have flow stresses that are independent of strain rate. In contrast, thermally activated processes exhibit flow stresses that decrease with increasing temperature and decreasing strain rate.[14] In Eq. (b) of Table 1, f^+ is the frequency and u^+ is the activation energy for the forward motion of dislocations. The amount of energy u^+ that must be supplied by thermal fluctuation in order to activate the process depends strongly on the applied stress τ; usually u^+ also depends on the dislocation substructure *str* and only mildly on the temperature T. The net strain rate is obtained by taking the difference between the forward (+) and reverse (−) rates.

Suzuki Locking of Dislocations

Suzuki solute-atom locking of dislocations is an interesting example of an athermal process.[17] The atomic arrangements of atoms on successive (111) planes in *FCC* crystals, as shown in Fig. 8, follow the sequence *ABCABC*, etc. The total slip Burgers vector b, however, will dissociate into a pair of Shockley partials as shown by Eq. (a) of Fig. 8, because the total energy decreases as a result of this reaction as calculated in Eq. (b) of Fig. 8. When this dissociation occurs, the new arrangement in Fig. 9 is obtained. The two Shockley partials are AA' having a Burgers vector b_1, and BB' having a Burgers vector b_2. Whereas to the left of AA' and to the right of BB' the atoms have the normal sequency of layering for the *FCC* system, between the two Shockley partials they have the sequence $C|AC|ABC$, etc., and thus exhibit a stacking fault. Since the sequence *CACACA*, etc., is that for the layering of successive basal planes in the hexagonal *CP* system, the stacking fault consists of two layers of atoms based on the hexagonal lattice. Since the *FCC* system is the more stable, the free energy of the crystal increases as the partials separate to greater distances. A minimum total free energy change is encountered at an equilibrium distance of separation d. An analogous situation occurs on the basal plane of hexagonal *CP* metals, where now the stacking fault consists of two layers of atoms arranged in the *FCC* sequence.

Suzuki showed that, when a binary alloy is hot enough (e.g., above about 0.4 of the melting temperature) so that diffusion can occur, the solute element will distribute itself between the surrounding ideal crystal and the stacking fault as demanded in all two-component two-phase equilibria. Under these conditions the situation shown in Fig. 10 will prevail. A composition c_f of the solute atoms will be obtained in the stacking fault, whereas the composition in the sound part of the crystal will remain nearly the average composition c. If a unit length of each partial dislocation is

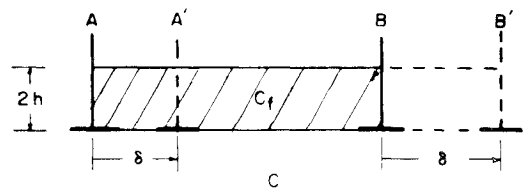

Fig. 10 Movement of dislocations in Suzuki located alloy.

moved a distance δ by an applied stress τ, the work done is $\tau b\delta$ and the volume $2h\delta$ is swept out by each partial dislocation, where h is the height of each atomic layer. As dislocation A moves to A', the increase in free energy is $2h/V(F_{c_f} - F_{c_f}{}^f)$, where V is the molar volume, and F_{c_f} and $F_{c_f}{}^f$ are the free energies at composition c_f of the ideal crystal and the fault, respectively. Similarly, the motion of the partial dislocation from B to B' requires an increase in free energy of $2h/V(F_c{}^f - F_c)$. Since the work done by the stress mechanically must account for the total increase in chemical free energy,

$$\tau = 2h/bV\{(F_c{}^f - F_c) - (F_{c_f}{}^f - F_{c_f})\} = 2h\Delta F/bV \quad (3)$$

where $2h/bV$ is well known from the crystal structure. The necessary thermodynamic data for obtaining the equilibrium composition and the free energies in the faulted region are not known, so that the deformation stress cannot yet be accurately calculated. Assuming, however, that both the ideal crystals and the faulted region are ideal solutions, it follows that, under equilibrium conditions,

$$c_f/(1 - c_f) = [c/(1 - c)]e^{-\Delta F/kT} \quad (4)$$

where

$$\Delta F = V/2h(\gamma_b - \gamma_a) \quad (5)$$

and where γ_b and γ_a are the stacking fault energies per square centimeter in the pure components b and a of the alloy. In this event,

$$\tau = (c - c_f)(\gamma_b - \gamma_a)/h \quad (6)$$

The work that must be done to unlock a Suzuki locked alloy can be quite high, and it cannot be supplemented by local thermal fluctuations. Therefore, the deformation stress changes with temperature only insofar as the temperature affects $\gamma_b - \gamma_a$, and Suzuki-locked alloys can maintain rather high flow stresses even up to temperatures approaching their melting point. The introduction of Suzuki locking might provide one of the bases for the development of engineering alloys that can maintain their lengths even at high temperatures.

To date, the only example of effective Suzuki locking which has been uncovered is for basal slip in the hexagonal phase of Ag containing 33 at.% Al. The variation of upper and lower yield strengths with temperature and strain rate is shown in Fig. 11. It is immediately apparent that changes in the shear strain rates from 10^{-4} to 10^4/sec do not materially affect the yield strength. Furthermore, in contrast to the usual trends, the upper yield strength increases as the temperature increases above about 0.4 of the melting temperature. These trends, wholly inconsistent Cottrell pinning of dislocations, are consistent only with those expected to Suzuki locked alloys. Assuming that Suzuki locking is operative in this alloy, the values of $\gamma_b - \gamma_a$ deduced from the upper yield strength data for the higher temperature range where equilibrium is maintained give reasonably good values for stacking fault energies, which vary almost linearly with temperature as expected.

Peierls Mechanism

This mechanism is a thermally activated process that is strain rate controlling for low-temperature plastic flow in

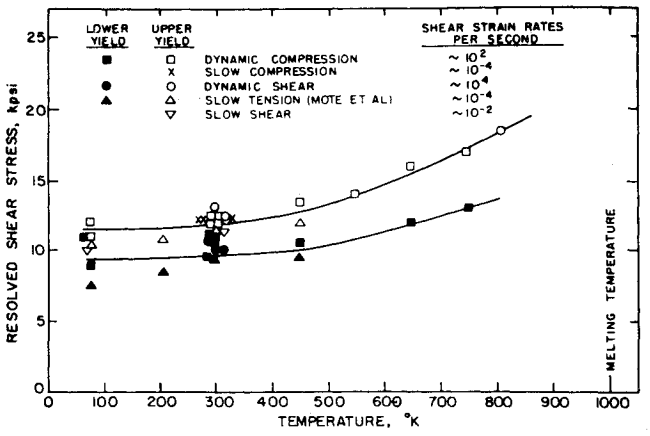

Fig. 11 Resolved shear stress vs temperature for basal slip of Ag (67%)-Al (33%) alloy.

BCC metals and for prismatic slip in hexagonal *CP* metals. The Peierls process has been discussed by Seeger,[18] Seeger, Donth, and Pfaff,[19] Lothe and Hirth,[20] and Friedel[21]; a brief outline of a more recent analysis by Dorn and Rajnak[22] is given below.

A dislocation has its lowest energy when it is in a valley parallel to a line of closely packed atoms as shown in Figs. 3a and 3b. As the dislocation moves from 3a to 3b, the bond angles and distances between atoms change and an increase in energy results. In *FCC* metals this energy increase is very small but is appreciable in *BCC* metals, which probably exhibit some covalent bonding. Although more general cases have been explored,[22] it is assumed here that the Peierls hill is sinusoidal (Fig. 12), with line energies per unit length of dislocation of Γ_c and Γ_0 at the hilltops and valleys, respectively. To move the dislocation as a unit over the Peierls hill at the absolute zero, a Peierls stress τ_p is required, and the maximum force per unit of the dislocation length is

$$\tau_p b = (\partial\Gamma/\partial y)_{y/a=\pi/2} = \pi/a(\Gamma_c - \Gamma_0) \tag{7}$$

When a stress $\tau < \tau_p$ is applied, the dislocation will advance part way up the Peierls hill to a position y_0 (Fig. 13), where the force to hold the dislocation at $y = y_0$ is

$$\tau b = (d\Gamma/\partial y)_{y_0} = -\pi/a(\Gamma_c - \Gamma_0)\sin(2\pi y_0/a) \tag{8}$$

The stress τ is the temperature-dependent contribution to the total flow stress. If τ_a is the applied stress and τ^* is the stress to overcome athermal mechanisms, $\tau = \tau_a - \tau^*$. At temperatures above the absolute zero, thermal fluctuations can assist the stress to locally bow out the dislocation (Fig. 13a). When the energy of a thermal fluctuation is great enough, a pair of kinks will be produced (Fig. 13b). Such kinks will then migrate under the applied stress to the geometric limits of the dislocation segment on which they formed. The frequency of nucleation of a pair of links, ν_n, in a length L is given by the Boltzmann condition:

$$\nu_n = (L/w)\nu_D e^{-u_n/kT} \tag{9}$$

where u_n is the saddle point energy required from a thermal fluctuation to form two kinks, k is the Boltzman constant, T is the absolute temperature, ν_D the debye frequency, L the length of dislocation, and w is about the length over which the critical fluctuation takes place. Then, in accord with the previous discussions, the shear strain rate is given by

$$\dot{\gamma} = \rho/L(La)(L/w)b\nu_D e^{-u_n/kT} \tag{10}$$

where ρ is the total length of dislocation per cubic centimeter, ρ/L is the number of lengths L, and La is the area swept out by the kink pair per successful fluctuation.

The value of u_n is equal to the increase in the line energy of a dislocation having a critical configuration for the nucleation of a pair of kinks. The increase in energy for a dislocation having any shape $y \equiv y\{x\}$ above that for one lying along $y = y_0$ (Fig. 14) is given by

$$u = \int_{-\infty}^{\infty} \left[\Gamma\{y\}\left\{1 + \left(\frac{dy}{dx}\right)^2\right\}^{1/2} - \Gamma\{y_0\} - \tau b(y - y_0)\right] dx \tag{11}$$

where the first term gives the line energy of the dislocation having a shape $y \equiv y\{x\}$, the second term gives the equilibrium line energy at $y = y_0$, and the third term is the work done by the stress during the displacement from y_0 to $y \equiv y\{x\}$. The minimum energy associated with the critical dislocation configuration is determined in terms of the calculus of variation by Euler's equation that

$$\begin{aligned}\partial/\partial y[\Gamma\{y\}\{1 + (dy/dx)^2\}^{1/2} - \Gamma\{y_0\} - \tau b(y - y_0)] = \\ d/dx\cdot\partial/\partial(dy/dx)[\Gamma\{y\}\{1 + (dy/dx)^2\}^{1/2} - \\ \Gamma\{y_0\} - \tau b(y - y_0)]\end{aligned} \tag{12}$$

which simplifies to

$$\tau b = d/dy[\Gamma\{y\}/\{1 + (dy/dx)^2\}^{1/2}] \tag{13}$$

Integrating once and applying the appropriate boundary conditions gives

$$\frac{dy}{dx} = \pm\left\{\frac{\Gamma^2\{y\} - [\Gamma\{y_0\} + \tau b(y - y_0)]^2}{[\Gamma\{y_0\} + \tau b(y - y_0)]^2}\right\}^{1/2} \tag{14}$$

which is the condition for the equilibrium kink shape of minimum energy. The critical solution of Eq. (14) occurs for $(y)_{x=0} - \lambda_c$ where $(dy/dx)_{x=0} = 0$, which requires that

$$\Gamma\{\lambda_0\} = \Gamma\{y_0\} + \tau b(\lambda_c - y_0) \tag{15}$$

Changing the independent variable in Eq. (11) from x to y and introducing Eq. (14) yields

$$u_n = u_{(\lambda_c)} = 2\int_{y_0}^{\lambda_c} (\Gamma^2\{y\}^2 - [\tau b\{y - y_0\} + \Gamma\{y_0\}]^2)^{1/2} dy \tag{16}$$

which gives u_n as a function of τ.

At a critical temperature T_c, $\tau = 0$, and the total energy for kink nucleation which is supplied by the thermal fluctuation is from Eq. (11), $u_{n(T_c)} = 2u_K$, where u_K is the energy of a single isolated kink; also at T_c, Eq. (20) yields

$$\dot{\gamma} = \rho/L(La)(L/w)b\nu_D e^{-2u_K/kT} \tag{17}$$

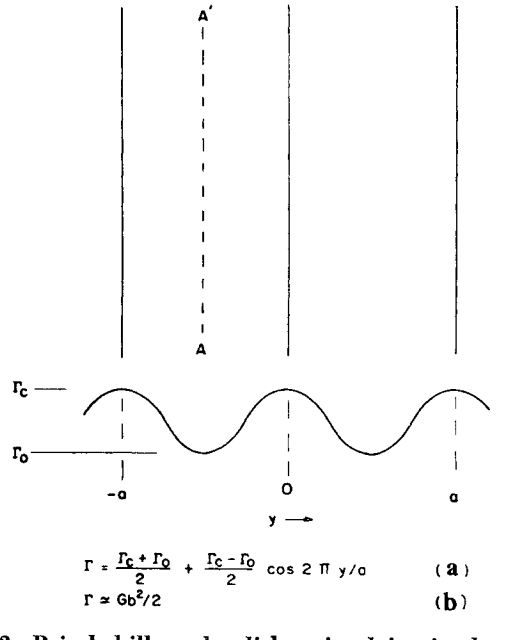

Fig. 12 Peierls hills and a dislocation lying in the valley.

Within the temperature range $0 \leq T \leq T_c$, where Eq. (10) is valid,

$$u_n/2u_K = T/T_c \tag{18}$$

as is seen by comparing Eqs. (10) and (17). Numerical integration of Eq. (16) is given in Fig. 15, which shows how the flow stress should vary with temperature for this idealized formulation of the Peierls process. The experimental datum points for the Ag-Al alloys (region I, Fig. 16) are in excellent agreement with the theoretically predicted curve deduced from Fig. 15.

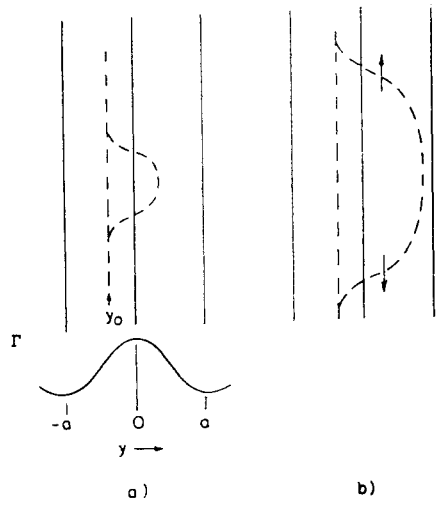

Fig. 13 The nucleation of a pair of kinks.

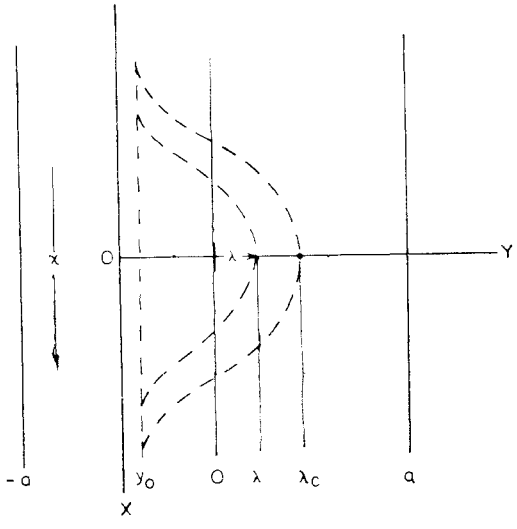

Fig. 14 Configurations during the nucleation of a pair of kinks.

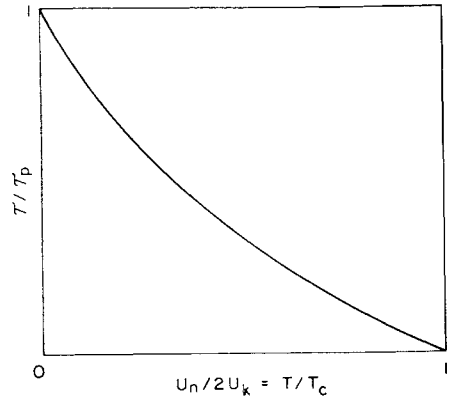

Fig. 15 Effect of stress on the energy to nucleate a pair of kinks.

Many important details of low-temperature plastic behavior of refractory *BCC* metals can be correlated in terms of theory. For example, the almost horizontal portion of the stress vs temperature curve for W as the temperature approaches zero represents not plastic flow but fracturing. As shown in Eq. (17), a decrease in $\dot{\gamma}$ or an increase in ρ would result in a lower value of T_c and therefore a lower brittle-to-ductile transition temperature. The value of ρ might be increased by small plastic deformations in the ductile region. Metals having higher shear moduli and higher Peierls hills will be more susceptable to low-temperature brittleness. Since the flow stress can now be analyzed in terms of the Peierls theory, half of the theory for brittle fracturing is known; the remaining part concerns the effect of various factors on the fracture stress.

Plastic Waves

All mathematical theories for plastic wave propagation, which are extensions of the classical theory developed independently by von Kármán[23] and Taylor,[24] are based on the equations for conservation of momentum and on the conditions for continuity. For the simple case of a plastic wave moving down a very thin rod, these equations are given in Table 2.

Equations (a1) and (a2) of Table 2 reveal that the velocity of a shock along the rod is

$$\partial\alpha/\partial t = \{[\sigma]/\rho[\epsilon]\}^{1/2} \tag{19}$$

Since there are three dependent variables (σ,ϵ,v) Eqs. (a) and (b) of Table 2 must be solved simultaneously with a third equation which describes the plastic behavior of the rod material. In their development von Kármán and Taylor assumed the deformation stress to be an exclusive function of the strain. Dissecting a finite shock into a series of small shocks such that $[\sigma]/[\epsilon]$ for each small shock approximates $\partial\sigma/\partial\epsilon$, the shock velocity becomes

$$\partial\alpha/\partial t = [(\partial\sigma/\partial\epsilon)/\rho]^{1/2} \tag{20}$$

Therefore, at stress levels below the yield stress the elastic wave velocity is $(E/\rho)^{1/2}$, where E is Young's modulus, whereas plastic waves are predicted to have slower velocities, since $\partial\sigma/\partial\epsilon$ in the plastic region is less than E. The only debatable issue in the original theory concerns the assumption that the deformation stress is an exclusive function of strain independent of time. The answer to this question for plastic waves in crystalline materials must be sought in terms of the behavior of dislocations.

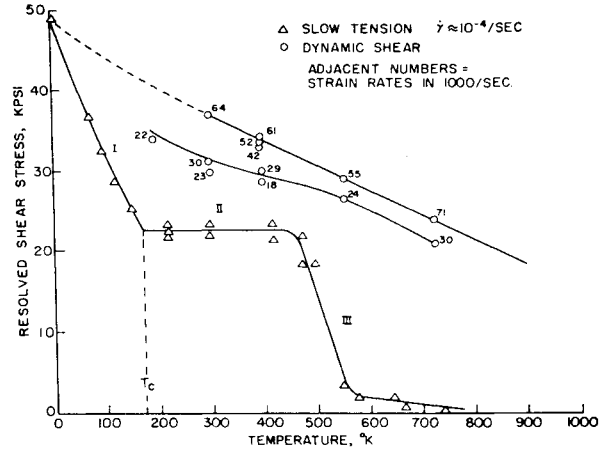

Fig. 16 Prismatic yielding vs temperature in Ag (67%)-Al (33%) alloy.

Table 2 Equations for plastic wave propogation in a thin rod

	Continuous variations	Hugoniot shock conditions
Condition for continuity	$\partial\epsilon/\partial t = \partial v/\partial\alpha$ (a1)	$[\epsilon]\partial\alpha/\partial t = -v$ (b1)
Conservation of momentum	$\partial\sigma/\partial\alpha = \rho(\partial v/\partial t)$ (a2)	$[\sigma] = -\rho[v]\partial\alpha/\partial t$ (b2)

where

ϵ = axial engineering strain
t = time
v = particle velocity
α = Lagrangian coordinate along rod axis
σ = axial engineering stress
ρ = density
[ ] = a shock in the bracketed value

Frank[25] has shown that the line energy of a dislocation increases with its velocity. A screw dislocation moving with a velocity v has a line energy given by the relativistic-like equation

$$\Gamma_v = \Gamma_0/\{1 - (v/c)^2\}^{1/2} \tag{21}$$

where Γ_0 is the rest energy of the dislocation and c is the elastic shear wave velocity in the crystal. Several important deductions result. The energy of a dislocation becomes infinite at velocities approaching the speed of sound. Unless certain special conditions prevail, the dislocation velocity cannot exceed the speed of sound. Dislocations have inertia; for example, expanding Eq. (13) into a Taylor's series reveals that a slow-moving dislocation has an effective mass Γ_0/c^2.

When a stationary dislocation is subjected to a shock in stress, it will immediately begin to accelerate, but since it has inertia it will not experience an instantaneous displacement. Therefore, no shock in plastic strain is possible, and Eq. (20) is, in general, invalid. The shock in total strain is exclusively the shock in elastic strain, and the wave will travel down the bar with the speed given by Eq. (19). This deduction is consistent with the experimental facts reported by Sternglass and Stewart,[26] Alter and Curtis,[27] and Riparbelli.[28]

The fact that dislocations have inertia suggests that under shock loading it will be necessary to account for the acceleration of dislocations in terms of the applied stress. Neglecting velocity sensitive dissipative mechanisms, the accelerative period can be estimated by equating the rate at which work is done on a moving dislocation to the increase in line energy.

Accordingly,

$$(\tau - \tau^*)bv = \partial\Gamma/\partial t \tag{22}$$

where τ^* is the stress where the dislocation will move against long-range stress fields. Integrating Eq. (22), letting $v = 0$ at $t = 0$, gives

$$(\tau - \tau^*)bct = \Gamma_0 v/c^2[1 - (v/c)^2]^{1/2} \tag{23}$$

Introducing values appropriate for Al, namely $c = 5 \times 10^{-5}$ cm/sec, $b = 2.86 \times 10^{-8}$ cm, and $\Gamma_0 = Gb^2/2 = 1.1 \times 10^{-4}$ erg/cm, the dislocation will reach a velocity of $0.9C$ in 2×10^{-11} sec for a small stress of 10^8 dyne/cm^2. The shear strain at this time is given by

$$\gamma = \int_0^{2 \times 10^{-11}} \rho' bv dt = 1.4 \times 10^{-4} \tag{24}$$

where ρ' is the density of moving dislocations taken to be 10^8/cm^2. Obviously, the dislocation accelerates to its limiting velocity in an extremely brief period of time, and the plastic strain during this period is also extremely small. Consequently, the formulation for the dynamic plastic behavior of crystalline materials need take into account strain rate changes only when information is needed for times less than 10^{-4} sec and for plastic strain less than about 10^{-4}.

For most analyses on plastic wave propagation, interest centers about longer times and larger plastic strains than those occurring during the accelerative period, and time need only be considered to the first-order terms of $\partial\gamma/\partial t$. Some dislocation processes that depend on time to the first-order magnitude are listed under classes 2 and 3 in Table 1. A typical example of the large effects of strain rate on the flow stress is shown in Fig. 16.[29–33] The data for slow strain-rate tests reveal three regions where different deformation processes are stress controlling. The thermally activated Peierls process is operative over region I, whereas over region II the athermal short-range order mechanism controls the flow stress, and in region III a thermally activated diffusion process is strain-rate controlling. Under dynamic testing, however, the upper temperature limit of the Peierls mechanism T_c is shifted to higher temperature. Furthermore, the times are so short under dynamic test conditions that no plastic strain can result at the higher temperatures from the diffusion-controlled mechanism. Consequently, at sufficiently high strain rates only the Peierls mechanism operates in this example.

The von Kármán assumption that $\sigma = \sigma\{\epsilon\}$ is useful only in a few cases where dislocation processes are insensitive to the strain rate, for example, due to short-range ordering. Such athermal strain rate-insensitive processes are usually accompanied by low-temperature thermally activated mechanisms, which, as previously discussed, replace the athermal mechanism under high strain-rate conditions. If, however, no low-temperature thermally activated mechanism operates (Fig. 11), the plastic behavior remains athermal and insensitive to strain rate for all test conditions. Only when these stringent conditions are met is the von Kármán assumption that $\sigma = \sigma\{\epsilon\}$ a reasonable approximation to the facts. For all other cases, the strain-rate-sensitive theories of plastic wave propagation should be employed.

Concluding Remarks

Whereas dislocation concepts and theory are now being employed toward the development of new and better engineering alloys, the great impact of dislocation theory on engineering has resulted principally from the correlated and unified philosophical approach it has given engineers toward the understanding of the mechanical behavior of materials. The author has attempted to set forth several items of research progress of personal interest in order to illustrate how dislocation theory works and how dislocations permit a description of plastic behavior in terms of the motion of lines of elastic discontinuities in crystals. Thus, dislocation theory is, in some respects, only a modest extension of the elasticity theory that is so familiar to engineers.

It appears that any engineer whose work impinges upon the behavior of materials is handicapped if he does not have at least a modest background in dislocation theory. When the few examples of deductions and correlations of mechanical behavior, given in the text of this report, are supplemented with the full scope of the application of dislocation theory to engineering, the great utility of the theory to many types of problems becomes ever more apparent.

As must be evident from the context of this report, dislocation theory need not be extremely esoteric or complex. Every engineer has the essential mathematical, physical, and chemical background to understand and become familiar with dislocations.

References

[1] Prandtl, L., "Hypothetical model for the kinetic theory of solid bodies," Z. Angew. Math. Mech. **8**, 85–96 (1928).

[2] Dehlinger, U., "Zur Theorie der Rekiestallisationreiner Metalle," Ann. Physik **2,** 749–793 (1929).

[3] Taylor, G. I., "The mechanism of plastic deformation of crystals, Part I, Theoretical," Proc. Royal Soc. (London) **A145,** 362–387 (1934).

[4] Orowan, E., "Zur Kristallplastizitat III, Uber den Mechanismus Gleitvorganges," Z. Physik. **89,** 634–659 (1934).

[5] Polanyi, M., "Uber eine Art Gitterstörung die einen Kristall plastisch machen könute," Z. Physik **89,** 660–664 (1934).

[6] Volterra, V., "Sur l'eguilibre des corps élastegues muttiplement connexes," Paris, Ann. Ec. Norm. **(3)24,** 401–426 (1907).

[7] Nabarro, F. R. N., "Mathematical theory of stationary dislocations," Advan. Phys. **1,** 269–394 (1952).

[8] Eshelby, J. D., "The continuum theory of lattice defects," Solid State Phys. **3,** 79–144 (1956).

[9] Seeger, A., "Theorie der Gitterfehlstellen," Encyclopedia Phys. **VII;** also Crystal Phys. **I,** 383–665 (1955).

[10] Kroner, E., *Kontinuumstheorie der Versetzung und Eigenspannung* (J. Springer, Berlin, 1958), pp. 18–45.

[11] Read, W. T., Jr., *Dislocations in Crystals* (McGraw-Hill Book Co. Inc., New York, 1953), Chap. 8, pp. 114–115.

[12] Cottrell, A., *Dislocations and Plastic Flow in Crystals* (Oxford University Press, New York, 1953), pp. 37–39.

[13] Friedel, J., *Les Dislocations* (Gaunthier-Villars, Paris, 1956).

[14] Dorn, J. E. and Mote, J. D., "Physical aspects of creep," Proc. Third Symp. Naval Structural Mech. (1963), to be published.

[15] Campbell, D., Simmons, J., and Dorn, J. E., "On the dynamic behavior of a Frank-Read Source," J. Appl. Mech. **83,** 447–455 (1961).

[16] Liebfried, G., "Uber den Einflub Thermisch angeregter Schwallweflen auf die plastische Deformation," Z. Physik **127,** 344–356 (1950).

[17] Suzuki, H., *Dislocations and Mechanical Properties of Crystals* (McGraw-Hill Book Co., Inc., New York, 1957), pp. 361–390.

[18] Seeger, A., "On the theory of the low-temperature internal friction peak observed in metals," Phil. Mag. **1,** 651–662 (1956).

[19] Seeger, A., Donth, H., and Pfaff, F., "The mechanism of low-temperature mechanical relaxation in deformed crystals," Discussions Faraday Soc. **23,** 19–37 (1957).

[20] Lothe, J. and Hirth, J. P., "Dislocation dynamics at low temperatures," Phys. Rev. **115,** 543–550 (1959).

[21] Friedel, J., *Electron Microscopy and Strength of Crystals* (Interscience Publishers Inc., New York, 1962), pp. 605–649.

[22] Dorn, J. and Rajnak, S., "Nucleation of kink pairs and the Peierls machinism of plastic deformation," Trans. AIME (to be published).

[23] von Kármán, T. and Duwez, P., "Propagation of plastic deformation in solids," J. Appl. Phys. **21,** 944–987 (1950).

[24] Taylor, G. I., "Plastic waves in wire extended by an impact load," *Scientific Papers I* (Cambridge University Press, New York, 1958), pp. 655–697.

[25] Frank, F. and Read, W., "Multiplication process for slow moving dislocations," Phys. Rev. **79,** 722–723 (1950).

[26] Sternglass, E. J. and Stewart, D. A., "An experimental study of the propagation of transient longitudinal deformation in elastoplastic," J. Appl. Mech. **20,** 427–434 (1953).

[27] Alter, B. E. K. and Curtis, C. W., "Effect of strain rate on the propagation of a plastic strain pulse along a lead bar," J. Appl. Phys. **27,** 1079–1085 (1956).

[28] Riparbelli, C., "On the relations among stress, strain and strain rate in copper wires submitted to longitudinal impact," Stress Analysis **14,** 55–70 (1954).

[29] Mote, J. D., Tanaka, K., and Dorn, J. E., "Effect of temperature on yielding in single crystals of hexagonal Ag-Al intermetallic phase," Trans. Met. Soc. AIME **221,** 858–866 (1961).

[30] Dorn, J. E. and Hauser, F. E., "Dislocation concepts of strain rate effects," Univ. Calif., Lawrence Radiation Lab. Rept. UCRL-10498 (September 1962).

[31] Dorn, J. E. and Rajnak, S., "Dislocations and plastic waves," Univ. Calif., Lawrence Radiation Lab. Rept. UCRL-10627 (March 1963).

[32] Howard, E., Barmore, W., Mote, J., and Dorn, J. E., "On the thermally-activated mechanism of prismatic slip in the Ag-Al hexagonal intermediate phase," Univ. of Calif., Lawrence Radiation Lab. Rept. UCRL-10588 (December 1962); also Trans. AIME (to be published).

[33] Larsen, T., Rajnak, S., Hauser, F. E., and Dorn, J. E., "Effect of strain rate and temperature on the yield strength of Ag-Al single crystals," Univ. Calif., Inst. of Eng. Res., Materials Res. Lab. Rept. Ser. 174, Issue 2 (July 1962).